SCALING MONTE CARLO KINETICS OF THE POTTS MODEL USING RATE THEORY

D. RAABE

Max-Planck-Institut für Eisenforschung, Max-Planck-Straße 1, 40237 Düsseldorf, Germany

Abstract—A method is introduced for scaling Monte Carlo kinetics of the Potts model using rate theory. The method is particularly designed for the kinetic and spatial scaling of multistate kinetic Potts models using one or more sets of non-conserved structural or orientational state variables S_i each of which can assume a number of Q_i degenerate ground states (Q or multistate Potts models) as commonly employed for simulating recrystallization and curvature driven grain growth phenomena. The approach is based on the equivalence of single-site state switches in the Potts model and grain boundary motion as described by Turnbull's classical rate theory mapped on a simulation lattice. According to this approach the switching probabilities can be scaled by the ratio of the local and the maximum occurring values of the grain boundary mobility and by the ratio of the local and the maximum occurring values of configurational and scalar contributions to the driving force. The real time step elapsing during one Monte Carlo time step is scaled by the maximum occurring grain boundary mobility, the maximum occurring driving force, and the lattice parameter of the simulation grid. © 2000 Acta Metallurgica Inc. Published by Elsevier Science Ltd. All rights reserved.

1. INTRODUCTION

Computer simulations which use time and space as independent variables are useful tools for investigating recrystallization and grain growth phenomena.

Applying them to spatially homogeneous starting microstructures allows one to examine analytical approaches and complement them with respect to topological aspects. Applying them to spatially non-homogeneous starting microstructures allows one to identify critical conditions and mechanisms that entail kinetic and topological deviations from analytical predictions. The latter aspect is of particular importance because non-homogeneous microstructures are the rule and not the exception in real materials.

Monte Carlo simulations based on the multistate kinetic Potts model have dominated the field of discrete recrystallization and grain growth predictions since their first introduction into physical metallurgy 15 years ago. Applications were devoted to normal grain growth [1–8], nucleation and static primary recrystallization [5–13], dynamic recrystallization [14, 15], abnormal grain growth [6–8, 16, 17], and growth processes under the influence of particle pinning [18–20].

The success of the Potts model can be attributed to its enormous flexibility, its computational simplicity, and the comparably short calculation times. An important shortcoming of the Potts model is the absence of intrinsic microstructural scaling measures.

The introduction of spatial and kinetic scaling into the Potts model offers two major advantages. First, it allows one to quantify space and time. This aspect is of relevance when aiming at the simulation of industrial processes, i.e. at the use of realistic boundary conditions. Second, the quantitative incorporation of a wide spectrum of realistic or experimental microstructure data, such as stored energy or grain boundary mobility and energy data, can only be realized on the basis of a *common* time and space scale. For instance, the presence of grain boundaries with different mobility but identical driving force should lead to different switching rates in the Potts model without spoiling the overall time scale of the simulation. This aspect is of relevance since experimental grain boundary mobility and energy data are increasingly available [21–24].

The introduction of scaling into mesoscale Monte Carlo simulations requires the combination of the underlying Potts lattice model with some adequate physical model of the situation to be investigated.

This paper suggests a method to scale Monte Carlo kinetics of the Potts model using rate theory. The scaling method is based on the equivalence of single-site state switches in the Potts model and grain boundary motion as described by classical rate theory mapped on a simulation lattice. The method is particularly designed for Potts models using a non-conserved structural state variable S (e.g. crystal orientation) which can assume a discrete number of Q degenerate ground states (Q or multistate Potts model). The method enables one to scale the switching probabilities by the ratio of the local and the maximum occurring values of the grain boundary mobility and by the ratio of the local and the maximum occurring values of configurational and scalar contributions to the driving force. The real time step elapsing during one Monte Carlo time step is scaled by the maximum occurring grain boundary mobility, the maximum occurring driving force, and the lattice parameter of the simulation lattice.

The plan of the paper is as follows. Section 2 is devoted to classical Monte Carlo kinetics of the multistate Potts model, reviewing in particular the energy operator, the Monte Carlo algorithm, classical Monte Carlo kinetics, and previous scaling approaches. Section 3 deals with classical rate theory of grain boundary motion. These two ingredients are used in Section 4 to derive the scaling method by formulating the equivalence of switches in the Potts model and grain boundary motion as quantified by rate theory.

2. MONTE CARLO KINETICS OF THE MULTISTATE POTTS MODEL

2.1. The energy operator

The Hamiltonian commonly used in Potts models [25] for simulating recrystallization and curvature driven grain growth typically quantifies the interfacial energy between dissimilar neighbor sites and the stored elastic energy [6–8, 11]

$$E = E_{gg} + E_{el}$$

$$= \sum_{i=1}^{N} \left\{ \frac{J}{2} \sum_{j=1}^{nnn} (1 - \delta_{S_i S_j}) + H_{el} f(Q_u - S_i) \right\} \quad (1)$$

where E_{gg} is the energy proportional to the total grain boundary energy in the system, E_{el} the energy proportional to the total elastic energy due to stored dislocations in the system, N the number of lattice sites, nnn the geometrically weighted number of neighbor sites in the first, second, and third neighbor shell, S the orientational state variable, $\delta_{S_i S_j}$ the Kronecker symbol which assumes a value of one if $S_i = S_j$ and a value of zero if $S_i \neq S_j$, J an energy proportional to the grain boundary energy, and H_{el} an energy proportional to the stored elastic

energy. J and H_{el} are positive. Their respective proportionality factors relating them to realistic energies scale the simulation with respect to thermal fluctuations. The ratio between the two proportionality factors determines the balance between curvature driven grain growth and recrystallization [11]. The function $f(Q_u - S_i)$ describes whether a site is recrystallized or not. Further details about the operator are given in Ref. [11].

The use of a spectrum of orientational states, each representing a discrete crystallographic orientation, allows one to map domains as regions of identical state, i.e. as crystal grains or subgrains. Equation (1) distinguishes configurational contributions to the energy, which are calculated as a sum over the immediate neighborhood nnn, from scalar contributions to the energy. This difference in the calculation of the system energy is of importance for the equivalence scaling procedure discussed later in this article.

2.2. Monte Carlo algorithm

The basic setup of a Monte Carlo model for simulating recrystallization and curvature driven grain coarsening consists of a spatial grid where the state of each lattice point is described in terms of a value of the orientational state variable (generalized spin) and a value of the scalar energy stored with this point (e.g. elastic energy due to stored dislocations). The configurational energy change is calculated during a trial flip of the orientational state variable by summing overall bonds between dissimilar neighbor points before and after the switch.

After mapping some initial configuration of these two state variables on a discrete spatial grid the Monte Carlo algorithm works according to the following rules. In the first step, a lattice coordinate is selected at random. In the second step, the values of the two state variables at this site are switched. In the third step, the total change in system energy associated with this switch is calculated applying equation (1) before and after the flip. In the fourth step, the probability that the chosen spin will switch is calculated using the Glauber transition function [26] or the Metropolis transition function [27]. The heat-bath method suggested by Glauber dynamics uses

$$W_{Gl} = \left(1 + \exp\left\{ -\frac{\Delta E}{k_B T} \right\} \right)^{-1} \quad (2)$$

with $\Delta E = E_n - E_o$, where E_n is the new total energy of the spin configuration after the trial switch, E_o the old total energy of the current spin configuration before the trial switch, W_{Gl} the Glauber switching probability, k_B the Boltzmann constant, and T the absolute temperature (Fig. 1). The Metropolis method (Fig. 2) uses a switching probability W_M according to
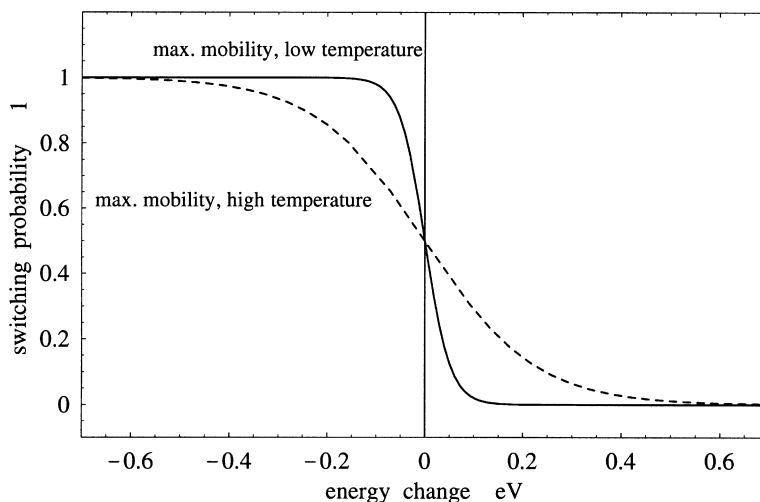
Fig. 1. Single-site Glauber transition function. The dashed line indicates high temperature and the solid line low temperature, equation (2).

$$W_{\mathrm{M}} = \begin{cases} \exp\left\{ -\dfrac{\Delta E}{k_{\mathrm{B}}T} \right\} & \text{if } \Delta E > 0 \\ 1 & \text{if } \Delta E \le 0 \end{cases} \qquad (3)$$

where $\Delta E = E_{\mathrm{n}} - E_{\mathrm{o}}$. In the fifth step, a random number ξ is generated in the interval $0 \le \xi < 1$. In the sixth step, the switching decision is made, i.e. the flip is accepted if ξ is equal or below the calculated Glauber or Metropolis switching probability. Otherwise the switch is rejected and the initial spin configuration remains unchanged. Further details about the Monte Carlo rules are given in the papers cited in Section 1.

2.3. Classical Monte Carlo kinetics

Monte Carlo kinetics are commonly quantified by defining N trial flips, where N is the number of lattice sites, as one Monte Carlo step, i.e.

$$\Delta t_{\mathrm{MC}} = \frac{n}{N} \qquad (4)$$

where Δt_{MC} is the Monte Carlo time step and n the number of trial switches. It is worth noting that this measure does not have the unit of time [s] but the unit of Monte Carlo steps [MCS].

At low temperatures, high degeneracy (high number of discrete possible states Q), and large average grain sizes (measured in units of lattice points), the probability of successfully switching an arbitrary site to a new orientation is very small and the Metropolis method becomes ineffective. For this reason Sahni et al. [28] and later Hassold and Holm [29] modified the continuous time method intro-
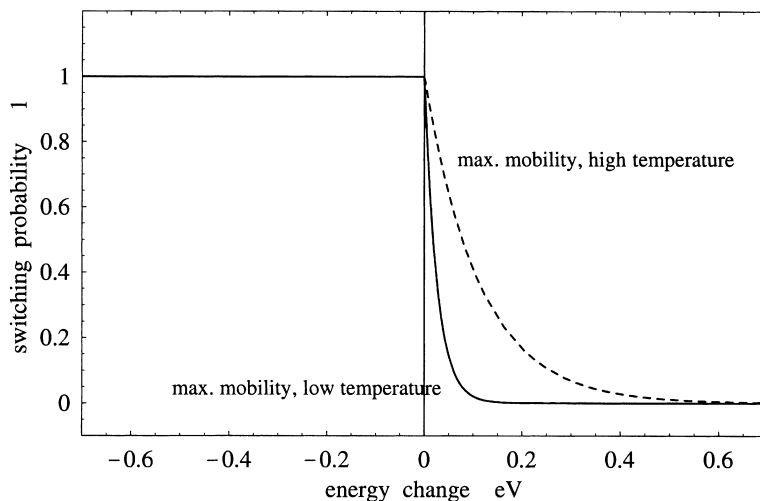

Fig. 2. Single-site Metropolis transition function. The dashed line indicates high temperature and the solid line low temperature, equation (3).

duced earlier for the Ising model [30] for the Potts model

$$\Delta t_{\text{MC}}^{\text{C}} = -\frac{(Q-1)\tau}{A}\ln(R) \tag{5}$$

where $\Delta t_{\text{MC}}^{\text{C}}$ is the Monte Carlo time step in the continuous time approach, Q the maximum number of discrete orientational states (spins), τ the average time between succeeding attempted state flips on the same lattice point (τ is usually regarded as the elementary Monte Carlo time unit), R a random number between zero and one, and A the total system activity which is defined by

$$A = \sum_{i=1}^{N}\Pi_i = \sum_{j=1}^{Q}\sum_{i=1}^{N}\pi_{ij} \tag{6}$$

where Π_i is the activity of lattice site i, and π_{ij} the probability of successfully flipping lattice site i to a new orientation S_j.

Further progress along this line was recently made by Mehnert and Klimanek [31] who derived a state-normalized version of the continuous time simulation method which allows one to reformulate Monte Carlo kinetics with a weaker dependence on the total number of possible orientational states

$$\Delta t_{\text{MC}}^{\mathcal{C}} = \frac{\Delta t_{\text{MC}}^{\text{C}}}{(Q-1)} = -\frac{\tau}{A}\ln(R) \tag{7}$$

where $\Delta t_{\text{MC}}^{\mathcal{C}}$ is the state-normalized Monte Carlo time step in the continuous time approach.

2.4. Previous scaling approaches

The major question in this paper is whether and how the above Monte Carlo time units [MCS] can be related to the real time [s]. In this context Safran et al. [32] suggested for atomic scale simulations to set the time scale by multiplying the transition probability with a basic attempt frequency $\Gamma = \tau_a^{-1}$. The authors assumed this attack frequency to have an Arrhenius-type temperature dependence†, i.e.

$$\Gamma = \frac{1}{\tau_a} = \exp\left\{-\frac{Q_a}{k_B T}\right\} \tag{8}$$

where Q_a is the activation energy associated with a single atomic jump event coupling the simulation to temperature. The Glauber transition probability according to Safran et al. then amounts to

$$W_{\text{Gl}}^{\text{S}} = \Gamma\left(1 + \exp\left\{-\frac{\Delta E}{k_B T}\right\}\right)^{-1}. \tag{9}$$

---

† Note that the original paper contains a misprint on p. 2695 concerning the sign of the argument of the exponential.

The Metropolis transition probability according to Safran et al. is

$$W_{\text{M}}^{\text{S}} = \begin{cases} \Gamma\exp\left\{-\dfrac{\Delta E}{k_B T}\right\} & \text{if } \Delta E > 0 \\ \Gamma & \text{if } \Delta E \leq 0. \end{cases} \tag{10}$$

Concerning mesoscale simulations of recrystallization and curvature driven grain coarsening Anderson et al. [1] and Srolovitz et al. [2] pointed out that the boundary velocity determined by tracking successive spin flips in the Potts model yields kinetics that are formally equivalent to the classical rate theory of boundary motion. Following the suggestion of Safran et al. [32], equation (8), the authors state that the conversion of Monte Carlo steps to real time has an implicit activation energy factor, $\exp\{-W_a/(k_B T)\}$, which corresponds to the atomic jump frequency.

Mehnert and Klimanek [31] recently suggested in their paper on the state-normalization of the continuous time method that a conversion of Monte Carlo time steps to real time should be feasible using

$$\Delta t_{\text{MC}}^{\mathcal{C}} = \theta\,\Delta t\,\nu_D\exp\left\{-\frac{W_{\text{gb}}}{k_B T}\right\} \tag{11}$$

where $\Delta t_{\text{MC}}^{\mathcal{C}}$ is the state-normalized Monte Carlo time step, Δt the real time step, ν_D the Debye frequency, θ a factor which correlates the physical to the model length scale, and W_{gb} the energy of activation for atom jumps from one grain surface through the boundary to the surface of the neighboring grain. This energy is usually termed the activation energy of grain boundary mobility.

Equations (5) and (7), discussed in the previous section, can also be regarded as scaling approaches. Though not generating a real time scale they introduce different Monte Carlo time weighting for sites with different switching probability. This means that a flip of a site with a small switching probability contributes a large portion to the Monte Carlo time step and vice versa.

A qualitative step forward in differentiating between switches associated with different mobilities of the grain boundaries involved was made by Holm et al. [33] [equation (8) in their paper]. For considering the influence of grain boundary mobility on the switching probability Holm et al. used a rule of the form

$$W_{\text{M}}^{\text{H}} = \begin{cases} 0 & \text{if } \Delta E > 0 \\ m & \text{if } \Delta E \leq 0 \end{cases} \tag{12}$$

where m is the mobility assigned to the switched site. It is important to note that this method introduces a relative switching rate of different sites provided different mobilities were assigned to them, rendering m into m_i. In their paper Holm et al. used

different spatial mobility functions in order to simulate microstructures with gradients in the resulting grain shape and size. A similar scaling method based on mobility was earlier used by Rollett *et al.* for the simulation of abnormal grain growth [17] [equation (4) in their paper].

3. PHENOMENOLOGICAL RATE THEORY OF GRAIN BOUNDARY MOTION

Turnbull formulated a phenomenological rate equation, which describes the motion of large angle grain boundaries in terms of isotropic single-atom diffusion processes perpendicular to a homogeneous planar grain boundary segment under the influence of free energy gradients

$$\dot{\mathbf{x}} = \mathbf{n}\nu_D\lambda_{gb}c\left(\exp\left\{-\frac{\Delta G - \Delta G_t/2}{k_B T}\right\} - \exp\left\{-\frac{\Delta G + \Delta G_t/2}{k_B T}\right\}\right) \quad (13)$$

where $\dot{\mathbf{x}}$ is the interface velocity, ν_D the Debye frequency, λ_{gb} the jump width through the interface, c the intrinsic concentration of in-plane self-diffusion carrier defects (e.g. grain boundary vacancies or shuffle sources), $\mathbf{n}$ the normal to the grain boundary segment, ΔG the Gibbs enthalpy of motion through the interface, ΔG_t the Gibbs enthalpy associated with the transformation, k_B the Boltzmann constant, and T the absolute temperature [34].

Bold symbols indicate vector quantities. The Debye frequency is of the order of 10^{13}–10^{14}/s and the jump width of the order of the magnitude of the Burgers vector.

Replacing the Gibbs enthalpy of motion by the corresponding enthalpy and entropy, expressing the concentration of the in-plane defects in terms of their thermal density, and expressing the Gibbs enthalpy associated with the transformation by the driving force and the activation volume leads to

$$\dot{\mathbf{x}} = \mathbf{n}\nu_D\lambda_{gb}\exp\left\{\frac{\Delta S_f}{k_B}\right\}\exp\left\{-\frac{\Delta H_f}{k_B T}\right\} \times \left(\exp\left\{-\frac{\Delta H_m - T\Delta S_m - (p\Omega/2)}{k_B T}\right\} - \exp\left\{-\frac{\Delta H_m - T\Delta S_m + (p\Omega/2)}{k_B T}\right\}\right) \quad (14)$$

where p is the negative change in Gibbs enthalpy per volume unit across the interface (driving force), Ω the atomic volume, ΔS_f the entropy of formation, ΔH_f the enthalpy of formation, ΔS_m the entropy of motion, and ΔH_m the enthalpy of motion. The atomic volume is of the order of b^3, where b is the magnitude of the Burgers vector.

While ΔS_f mainly quantifies the vibrational entropy, ΔS_m contains configurational and vibrational portions. Summarizing these terms leads to

$$\dot{\mathbf{x}} = \mathbf{n}\nu_D b\exp\left\{\frac{\Delta S_f + \Delta S_m}{k_B}\right\}\sinh\left(\frac{p\Omega}{k_B T}\right) \times \exp\left\{-\frac{\Delta H_f + \Delta H_m}{k_B T}\right\}. \quad (15)$$

Due to the small argument in the sinh, equation (15) can be linearized

$$\dot{\mathbf{x}} \approx \mathbf{n}\nu_D b\exp\left\{\frac{\Delta S_f + \Delta S_m}{k_B}\right\}\left(\frac{p\Omega}{k_B T}\right) \times \exp\left\{-\frac{\Delta H_f + \Delta H_m}{k_B T}\right\}. \quad (16)$$

This approximation reproduces the well-known phenomenological Turnbull expression

$$\dot{\mathbf{x}} = \mathbf{n}\,mp = \mathbf{n}\,m_0 \times \exp\left\{-\frac{Q_{gb}}{k_B T}\right\}p \quad (17)$$

where m is the mobility, m_0 the pre-exponential factor, and Q_{gb} the activation energy of grain boundary mobility.

Comparing the coefficients in equations (16) and (17) yields

$$m_0 = \frac{\nu_D b\Omega}{k_B T}\exp\left\{\frac{\Delta S_f + \Delta S_m}{k_B}\right\}$$

$$Q_{gb} = \Delta H_f + \Delta H_m. \quad (18)$$

Equations (13)–(18) provide a phenomenological kinetic picture of grain boundary motion, where the atomic processes associated with a particular grain boundary are statistically described in terms of $m = m_0(\Delta\mathbf{g}, \mathbf{n})$ and $Q_{gb} = Q_{gb}(\Delta\mathbf{g}, \mathbf{n})$, where $\mathbf{g}$ is the rotation matrix quantifying the misorientation across the grain boundary and $\mathbf{n}$ the normal of the grain boundary segment.

Considering the misorientation and the boundary normal of each grain boundary segment occurring in a microstructure simulation is of importance because of the strong dependence of the grain boundary mobility on these parameters. Since it is difficult to quantify some of the physical parameters in equation (18), particularly with respect to their dependence on the misorientation, it is preferable to use experimental rather than theoretical mobility data wherever possible [21–24].

4. SCALING BY EQUIVALENCE

4.1. General formulation

The lattice site flips occurring in a Potts model based on a Hamiltonian of the type shown in equation (1) for curvature driven grain growth and recrystallization implicitly mimic the motion of

grain boundary segments. This means that the classical linearized symmetric rate theory for thermally activated grain boundary motion under the influence of free energy gradients as outlined above, equation (17), is an appropriate kinetic model for expressing the equivalence of spin flips in the Potts model and real grain boundary motion. Formally, the equivalence can be expressed by

$$\dot{\mathbf{x}}_P = \dot{\mathbf{x}}_{rate}$$

$$\mathbf{n}\frac{\lambda_P}{\Delta t_{MC}\Delta t_{real}} = \mathbf{n}m(p_c + p_s)$$

$$\frac{\lambda_P}{\Delta t_{MC}\Delta t_{real}} = m_0 \exp\left\{-\frac{Q_{gb}}{k_B T}\right\}(p_c + p_s) \qquad (19)$$

where $\dot{\mathbf{x}}_P$ is the boundary velocity in the Potts model, $\dot{\mathbf{x}}_{rate}$ the boundary velocity according to rate theory as given by equation (17), $\mathbf{n}$ the normal of the grain boundary segment, p_c configurational contributions to the driving force (e.g. through boundary curvature), p_s scalar contributions to the driving force (e.g. through the elastic energy associated with stored dislocations or through an applied magnetic field), Δt_{MC} the kinetic Monte Carlo measure in units of [MCS] as given by equation (4), λ_P the jump width or lattice parameter of the Potts model in units of [m], and Δt_{real} the real time step in units of [s/MCS].

The separation of the configurational from the scalar contributions to the total driving force is necessary since the scaling introduced by equation (19) must be formulated for a single-site switching function of the type given by equation (2) or equation (3) rather than for a coupled set of differential equations of motion.

Reformulating equation (19) leads to an expression for the real time elapsing during a number of Δt_{MC} kinetic Monte Carlo time steps

$$\Delta t_{real} = \frac{\lambda_P}{\Delta t_{MC} mp}$$

$$= \frac{\lambda_P}{\Delta t_{MC} m_0(p_c + p_s)}\exp\left\{+\frac{Q_{gb}}{k_B T}\right\}. \qquad (20)$$

This equation shows that the real time step can only be expressed in units of [s/MCS]. For one single Monte Carlo time step ($\Delta t_{MC} = 1$ MCS) the real time step amounts to

$$\Delta t_{real} = \frac{\lambda_P}{mp} \quad \left[\frac{s}{MCS}\right]. \qquad (21)$$

This simple preliminary result is physically plausible because it is obvious that a large prescribed lattice spacing λ_P requires a large time step to be swept by a moving grain boundary while a fast boundary needs a small time unit to sweep a given length λ_P.

The inverse of this elementary time step can be regarded as an attack frequency $\Gamma_{real} = 1/\Delta t_{real}$ which is for a given lattice with parameter λ_P characteristic of a particular grain boundary.

Since the time scale introduced in equation (21) is thus dependent on the *local* grain boundary velocity at lattice point i, i.e.

$$\Delta t_{real}^i = \frac{\lambda_P}{m^i p^i} \quad \left[\frac{s}{MCS}\right] \qquad (22)$$

where $m = m^i$ is the local grain boundary mobility at lattice point i and $p = p^i$ the local driving force at lattice point i, equations (20) and (21) are only applicable to situations in which the driving force and the mobility are the same everywhere in the system. Such a restriction does only apply for a very limited number of highly idealized cases, for instance for primary static recrystallization in a perfect homogeneous single crystal with equal driving force (neglecting the influence of curvature) and equal grain boundary mobility throughout the entire specimen.

In a heterogeneous material, equation (21) would thus give a different characteristic time scale at different lattice points. Such a non-normalized scaling rule would be of no use. In order to adapt this scaling method to systems with a non-homogeneous distribution of driving force and mobility it is thus useful to normalize the system to a *common* time scale Δt_{real}^{min}.

Such a common time scale is identical to the minimum time scale occurring in the system. It is determined by the fastest moving grain boundary in the array. According to equation (17) the fastest possible grain boundary is characterized by maximum mobility m^{max} and maximum driving force p^{max}, changing equation (21) into

$$\Delta t_{real}^{min} = \frac{\lambda_P}{m^{max}p^{max}} = \frac{\lambda_P}{m_0^{max}(p_c^{max} + p_s^{max})}$$
$$\times \exp\left\{\frac{Q_{gb}^{min}}{k_B T}\right\} \quad \left[\frac{s}{MCS}\right] \qquad (23)$$

where m_0^{max} is the pre-exponential factor and Q_{gb}^{min} the activation energy associated with the grain boundary with the highest mobility in the system. Δt_{MC} was here set to one Monte Carlo time step.

Before using this minimum occurring time step as a common time basis for *all* possible cell flips the corresponding single-site transition functions, equations (2) and (3), must be normalized in accord with this measure. This means that they must be scaled by the ratio of the local and the maximum occurring values of the grain boundary mobility and driving force. The Glauber transition function then changes to

$$\hat{W}_{Gl} = \left(\frac{m^i}{m^{max}}\right)\left(\frac{p_c^{max} + p_s^i}{p_c^{max} + p_s^{max}}\right)\left(1 + \exp\left\{\frac{\Delta E}{k_B T}\right\}\right)^{-1}$$

(24)

where ΔE is $E_n - E_o$, equation (2), p_c^{max} the maximum configurational driving force, p_s^{max} the maximum scalar (i.e. magnetic or elastic) driving force, and p_s^i the *local* scalar driving force at lattice point i.

It is important to note in equation (24) that the mobility ratio (m^i/m^{max}) equally influences the forward and the backward motion of a grain boundary that may occur due to thermal fluctuation. This is plausible since for instance a twin boundary with a very small mobility can neither easily move according to the driving force nor fluctuate against it. In other words, the drag effect caused by low mobility principally acts in both directions. The effect of a mobility change according to equation (24) is shown in Fig. 3 for the Glauber function. Correspondingly, the Metropolis transition function changes to

$$\hat{W}_M =$$

$$\begin{cases} \left(\frac{m^i}{m^{max}}\right)\left(\frac{p_c^{max} + p_s^i}{p_c^{max} + p_s^{max}}\right)\exp\left\{-\frac{\Delta E}{k_B T}\right\} & \text{if } \Delta E > 0 \\ \left(\frac{m^i}{m^{max}}\right)\left(\frac{p_c^{max} + p_s^i}{p_c^{max} + p_s^{max}}\right) & \text{if } \Delta E \leq 0. \end{cases}$$

(25)

The effect of a mobility change according to equation (25) is shown in Fig. 4 for the Metropolis function.

Both scaled single-site transition functions predict a non-vanishing switching probability, $(m^i p_c^{max})/(m^{max}[p_c^{max} + p_s^{max}])$, for cases where the scalar driving forces are zero which is due to the ubiquitous presence of configurational driving forces.

Since the driving force term in equations (24) and (25) has the constant maximum configurational driving force and the local scalar driving force in the numerator and the constant maximum total (scalar and configurational) driving force in the denominator the maximum possible transition probability is exactly equal to one provided the local mobility is equal to the maximum mobility. The only situation where the transition probability at a lattice point is zero occurs when the local grain boundary mobility m^i is zero.

A comment must be made at this point about the relation between the energy change ΔE associated with each trial switch, equation (1), and the real driving forces that occur in the modified transition functions, equations (24) and (25). Energy changes given by the operator in equation (1) are not equivalent but only proportional to the negative driving forces (multiplied by the transformed volume unit). This means that the energy term ΔE in the transition functions serves exclusively to quantify the sensitivity of the system with respect to thermal fluctuations. The use of a Boltzmann-type penalty term for the evaluation of fluctuations can be regarded as a mathematical method to overcome
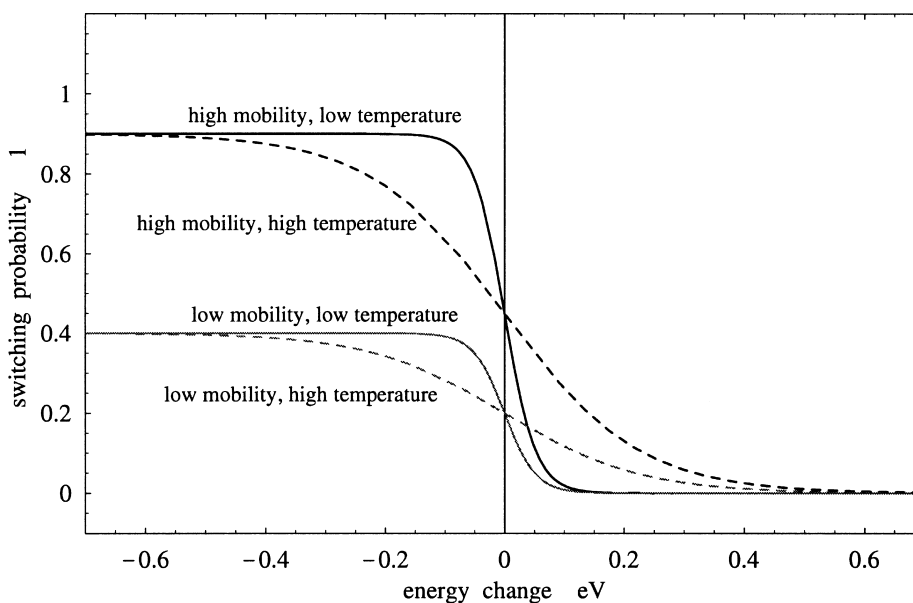

Fig. 3. Scaled single-site Glauber-type transition function for two different temperatures and grain boundary mobilities. The dashed lines indicate high temperature and the solid lines low temperature. The black lines indicate high mobility and the gray lines low mobility. The driving forces were constant, equation (24).

local energy minima that occur in Metropolis-type Monte Carlo simulations. True thermal fluctuations occur at an atomic scale. In the here suggested new concept they are already included in Turnbull's rate formulation of grain boundary motion, equation (13), which balances forward and backward jumps of the atoms through the boundary. This means that the true temperature dependence of recrystallization and grain growth dynamics lies in this framework in the temperature dependence of grain boundary motion which is fully accounted for by the activation energy of grain boundary mobility, equation (17).

Except for the use of thermal fluctuations, which are a typical feature of all Metropolis-type Monte Carlo methods, equations (19)–(25) reveal formal correspondence to the time scale and the transition functions derived for a probabilistic cellular automaton which is based on directly mapping rate theory on a simulation lattice [35].

4.2. Formulation for recrystallization and curvature driven grain growth

It is conceivable that various contributions $p_{j,s}^i$ may add to the total local scalar driving force on a grain boundary at lattice point i, i.e. $p_s^i = \sum_j p_{j,s}^i$. When using such different scalar driving forces in the scaled Monte Carlo algorithm, qualitative differences between them must be considered. While magnetic driving forces can occur on either side of

a fluctuating grain boundary, the use of a scalar driving force arising from elastic lattice distortions caused by stored dislocations ($p_s^i = p_{\rho,s}^i$) is not admissible for the quantification of thermal fluctuations since they may act *against* the sign of that force. The reason for this asymmetry is that it would violate the second law of thermodynamics if the stored internal energy would increase through the spontaneous accumulation of dislocations. In other words, stored dislocations are removed by a moving grain boundary but they cannot be formed by a fluctuating interface, i.e. by a trial flip. In contrast, magnetic energy terms must be considered both in the case of an energy increase and in the case of an energy decrease.

For simulations of recrystallization and curvature driven grain growth the Glauber switching function, therefore, is

$$
\tilde{W}_{Gl} = \begin{cases}
\left(\dfrac{m^i}{m^{\max}}\right)\left(\dfrac{p_c^{\max}}{p_c^{\max}+p_s^{\max}}\right)\left(1+\exp\left\{\dfrac{\Delta E}{k_B T}\right\}\right)^{-1} \\
\qquad\qquad \text{if } \Delta E > 0 \\[1.5em]
\left(\dfrac{m^i}{m^{\max}}\right)\left(\dfrac{p_c^{\max}+p_{\rho,s}^i}{p_c^{\max}+p_s^{\max}}\right)\left(1+\exp\left\{\dfrac{\Delta E}{k_B T}\right\}\right)^{-1} \\
\qquad\qquad \text{if } \Delta E \leq 0.
\end{cases}
$$

(26)

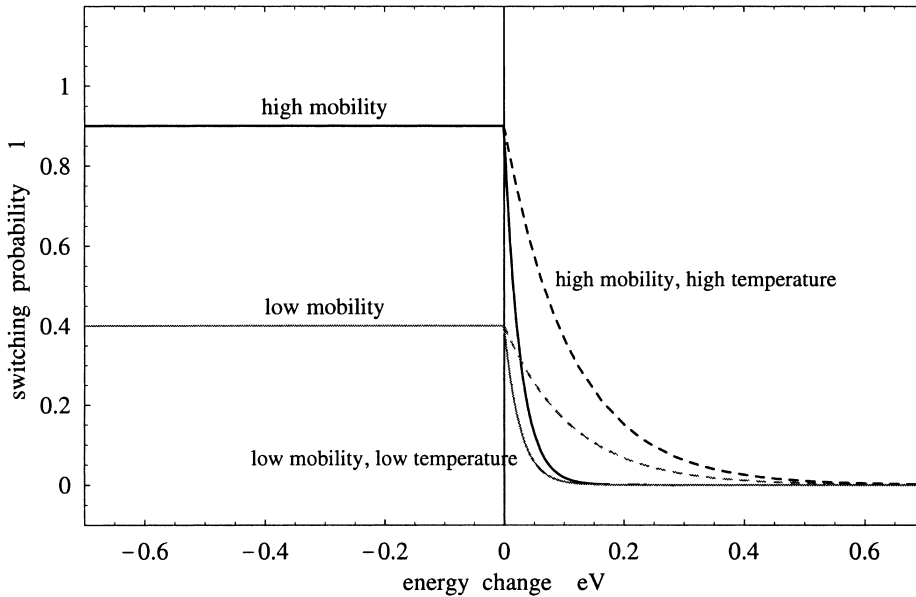The Metropolis transition function for this case is

Fig. 4. Scaled single-site Metropolis-type transition function for two different temperatures and grain boundary mobilities. The dashed lines indicate high temperature and the solid lines low temperature. The black lines indicate high mobility and the gray lines low mobility. The driving forces were constant, equation (25).
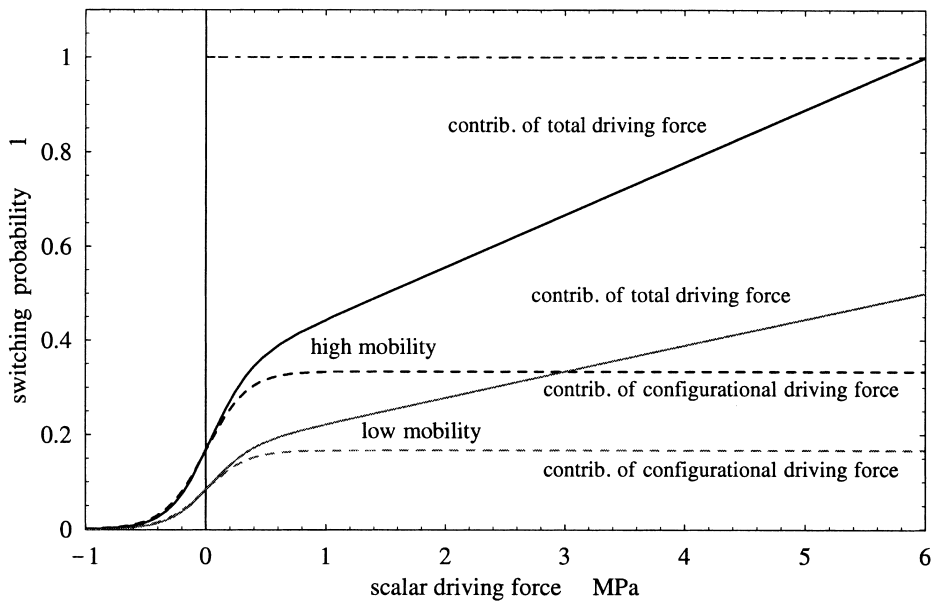
Fig. 5. Scaled single-site Glauber-type switching probability as a function of the scalar driving force for two different grain boundary mobilities. The dashed lines show the transition probability for configurational driving forces and the solid lines for the total driving force. The black lines indicate high mobility and the gray lines low mobility. The temperature was constant. The dashed line at $W = 1$ represents the maximum possible switching probability for cases with maximum grain boundary mobility and maximum scalar driving force ($p_s^{max} = 6$ MPa), equation (26).
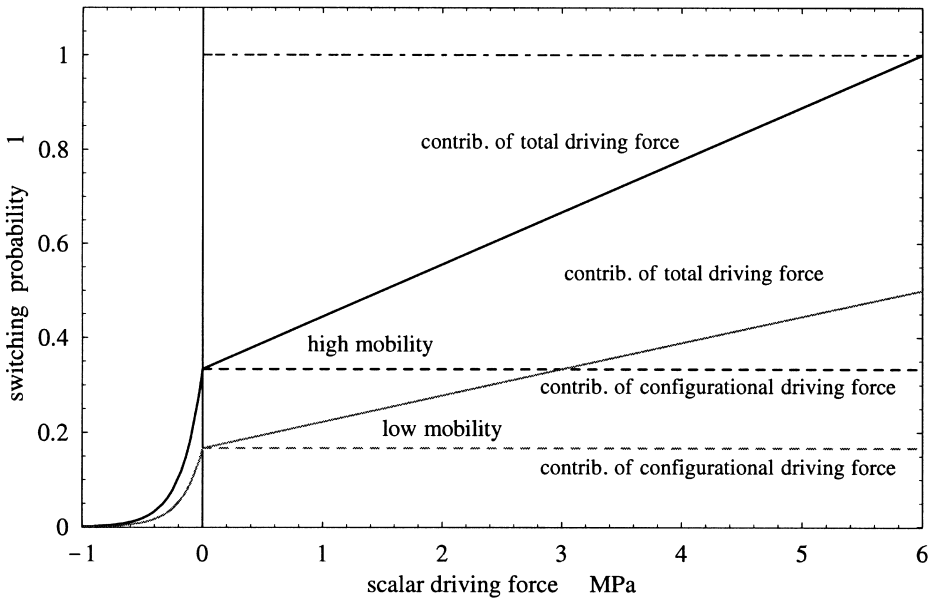

Fig. 6. Scaled single-site Metropolis-type switching probability as a function of the scalar driving force for two different grain boundary mobilities. The dashed lines show the transition probability for configurational driving forces and the solid lines for the total driving force. The black lines indicate high mobility and the gray lines low mobility. The temperature was constant. The dashed line at $W = 1$ represents the maximum possible switching probability for cases with maximum grain boundary mobility and maximum scalar driving force ($p_s^{max} = 6$ MPa), equation (27).
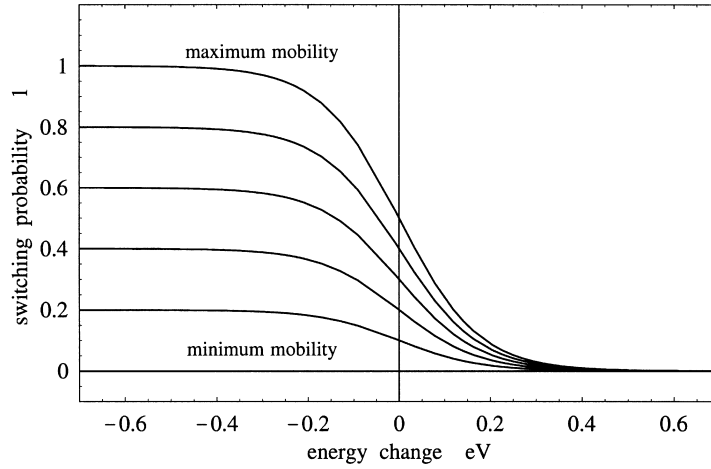
Fig. 7. Scaled single-site Glauber-type transition function for pure curvature driven grain growth at constant temperature for grain boundaries of different mobility. The transition probabilities are independent of the driving force, equation (28).

$$\tilde{W}_M =$$

$$\begin{cases} \left(\dfrac{m^i}{m^{max}}\right)\left(\dfrac{p_c^{max}}{p_c^{max} + p_s^{max}}\right)\exp\left\{-\dfrac{\Delta E}{k_B T}\right\} & \text{if } \Delta E > 0 \\[2ex] \left(\dfrac{m^i}{m^{max}}\right)\left(\dfrac{p_c^{max} + p_{\rho,s}^i}{p_c^{max} + p_s^{max}}\right) & \text{if } \Delta E \leq 0. \end{cases}$$

$$(27)$$

These modified single-site transition functions predict a switching probability different from zero even if all non-configurational local driving forces are absent. The transition probability is then exclusively due to configurational contributions. The driving force term in equations (26) and (27) has the constant maximum configurational driving force both in the numerator and in the denominator. For the

case of energy decrease the driving force term additionally contains the local scalar driving force in the numerator and the maximum scalar driving force in the denominator. This means that the maximum possible transition probability in the direction of the driving force is exactly equal to one if the local mobility is equal to the maximum mobility ($m^i = m^{max}$) and if at the same time the local scalar portion of the driving force is equal to its maximum possible value ($p_{\rho,s}^i = p_s^{max}$).

The only situation where the transition probability becomes equal to zero occurs for a local grain boundary which has zero mobility ($m^i = 0$). This is conceivable for small angle boundaries and certain twin boundaries. Figures 5 and 6 show the switching probability as a function of the local scalar driving force stemming from stored dislocations
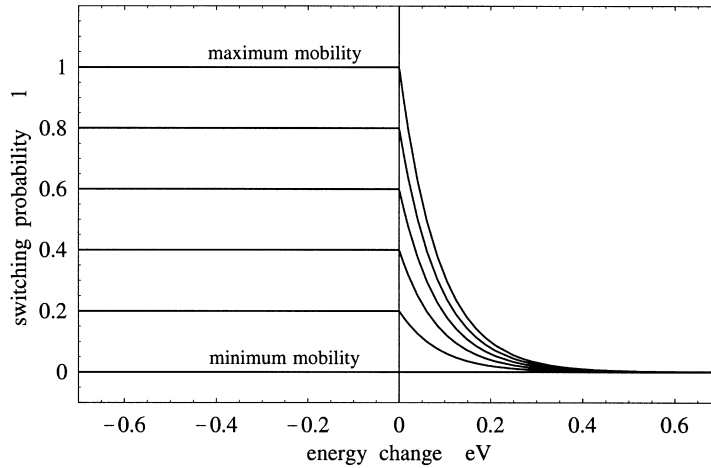

Fig. 8. Scaled single-site Metropolis-type transition function for pure curvature driven grain growth at constant temperature for grain boundaries of different mobility. The transition probabilities are independent of the driving force, equation (29).

$p^i_{\rho,s}$ for the scaled Glauber transition function and for the scaled Metropolis transition function according to equations (26) and (27).

4.3. Formulation for pure curvature driven grain growth

This section presents scaled versions of the above introduced switching probability functions for pure curvature driven grain growth simulations where no scalar contributions to the driving force occur.

The corresponding single-site switching functions can be derived from equations (26) and (27) by simply dropping the terms for the scalar driving force (Figs 7 and 8). The Glauber function then reduces to

$$\check{W}_{\text{Gl}} = \left(\frac{m^i}{m^{\max}}\right)\left(1 + \exp\left\{\frac{\Delta E}{k_{\text{B}}T}\right\}\right)^{-1}. \quad (28)$$

The Metropolis transition function for this case reduces to

$$\check{W}_{\text{M}} = \begin{cases} \left(\dfrac{m^i}{m^{\max}}\right)\exp\left\{-\dfrac{\Delta E}{k_{\text{B}}T}\right\} & \text{if } \Delta E > 0 \\[2ex] \left(\dfrac{m^i}{m^{\max}}\right) & \text{if } \Delta E \leq 0. \end{cases} \quad (29)$$

Equations (28) and (29) show that scaling for pure grain growth simulations can be obtained by simply multiplying the original single-site switching functions, equations (2) and (3), by the ratio of the local and the maximum values of the grain boundary mobility.

Monte Carlo simulations on the basis of the scaled Metropolis transition function for curvature driven grain growth, equation (29), have recently been conducted by Rollett [36, 37].

5. CONCLUSIONS

The paper introduced a method for scaling Monte Carlo kinetics of the Potts model using Turnbull's rate theory of grain boundary motion. The method is designed for the kinetic and spatial scaling of multistate Potts models using one or more sets of non-conserved discrete structural or orientational state variables as employed for simulating recrystallization and curvature driven grain growth phenomena.

The scaling is based on the equivalence of single-site state switches in the Potts model and grain boundary motion as described by rate theory mapped on a simulation lattice.

According to this method the switching probabilities can be scaled by the ratio of the local and the maximum occurring values of the grain boundary mobility and by the ratio of the local and the maximum occurring values of configurational and scalar contributions to the driving force. The real time step elapsing during one Monte Carlo time step is scaled by the maximum occurring grain boundary mobility, the maximum occurring driving force, and the lattice parameter of the simulation grid.

Various scaled Glauber- and Metropolis-type transition functions were derived and discussed with respect to applications in the fields of recrystallization and grain growth Monte Carlo simulations.

REFERENCES

1. Anderson, M. P., Srolovitz, D. J., Grest, G. S. and Sahni, P. S., *Acta metall.*, 1984, **32**, 783.
2. Srolovitz, D. J., Anderson, M. P., Sahni, P. S. and Grest, G. S., *Acta metall.*, 1984, **32**, 793.
3. Glazier, J. A., Anderson, M. P. and Grest, G. S., *Phil. Mag. B*, 1990, **62**, 615.
4. Mehnert, K. and Klimanek, P., *Comput. Mater. Sci.*, 1997, **9**, 261.
5. Mehnert, K. and Klimanek, P., in *Texture and Anisotropy of Polycrystals*, ed. R. Schwarzer. Trans Tech Publications, Switzerland, 1998, p. 425.
6. Srolovitz, D. J., *Computer Simulation of Microstructural Evolution*. The Metallurgical Society of AIME, Warrendale, PA, 1986.
7. Anderson, M. P. and Rollett, A. D., *Simulation and Theory of Evolving Microstructures*. The Minerals, Metals and Materials Society, TMS Publication, Warrendale, PA, 1990.
8. Holm, E. A., Rollett, A. D. and Srolovitz, D. J., in *Proceedings of NATO ASI on Computer Simulation in Materials Science*, ed. H. O. Kirchner, L. P. Kubin and V. Pontikis, *NATO Advanced Science Institutes Series, Series E, Applied Sciences*, Vol. 308. Kluwer Academic, Dordrecht, in cooperation with NATO Science Division, 1996, p. 373.
9. Tavernier, P. and Szpunar, J. A., *Acta metall.*, 1991, **39**, 549.
10. Tavernier, P. and Szpunar, J. A., *Acta metall.*, 1991, **39**, 557.
11. Srolovitz, D. J., Grest, G. S. and Anderson, M. P., *Acta metall.*, 1986, **34**, 1833.
12. Srolovitz, D. J., Grest, G. S., Anderson, M. P. and Rollett, A. D., *Acta metall.*, 1988, **36**, 2115.
13. Rollett, A. D., Srolovitz, D. J., Doherty, R. D. and Anderson, M. P., *Acta metall.*, 1989, **37**, 627.
14. Rollett, A. D., Luton, M. J. and Srolovitz, D. J., *Acta metall.*, 1992, **40**, 43.
15. Peczak, P., *Acta metall.*, 1995, **43**, 1297.
16. Srolovitz, D. J., Grest, G. S. and Anderson, M. P., *Acta metall.*, 1985, **33**, 2233.
17. Rollett, A. D., Srolovitz, D. J. and Anderson, M. P., *Acta metall.*, 1989, **37**, 1227.
18. Doherty, R. D., Li, K., Anderson, M. P., Rollett, A. D. and Srolovitz, D. J., in *Proceedings of the International Conference on Recrystallization in Metallic Materials, Recrystallization 1990*, ed. T. Chandra. The Minerals, Metals and Materials Society, TMS Publication, Warrendale, PA, 1990, p. 129.
19. Miodownik, M. A., in *Proceedings of the Third International Conference on Grain Growth, 1998*, ed.

H. Weiland. The Minerals, Metals and Materials Society, TMS Publication, Warrendale, PA, 1998.

20. Miodownik, M. A., Martin, J. W. and Cerezo, A., *Phil. Mag.*, 1999, **79**, 203.

21. Gottstein, G., Molodov, D. A., Czubayko, U. and Shvindlerman, L. S., *J. Physique IV, colloque C3, supplément au J. Physique III*, 1995, **5**, 9.

22. Shvindlerman, L. S., Czubayko, U., Gottstein, G. and Molodov, D. A., in *Proceedings 16th RISØ International Symposium on Materials Science: Microstructural and Crystallographic Aspects of Recrystallization*, ed. N. Hansen, D. Juul Jensen, Y. L. Liu and B. Ralph. RISØ National Laboratory, Roskilde, Denmark, 1995, p. 545.

23. Gottstein, G., Shvindlerman, L. S., Molodov, D. A. and Czubayko, U., in *Dynamics of Crystal Surfaces and Interfaces*, ed. P. M. Duxbury and T. J. Pence. Plenum Press, New York, 1997, p. 109.

24. Gottstein, G., Molodov, D. A. and Shvindlerman, L. S., *Interface Sci.*, 1998, **6**, 7.

25. Potts, R. B., *Proc. Camb. phil. Soc.*, 1952, **48**, 106.

26. Glauber, R. J., *J. Math. Phys.*, 1963, **4**, 294.

27. Metropolis, N., Rosenbluth, A. W., Rosenbluth, M. N., Teller, A. T. and Teller, E., *J. chem. Phys.*, 1953, **21**, 1087.

28. Sahni, P. S., Srolovitz, D. J., Grest, G. S., Anderson, M. P. and Safran, B. A., *Phys. Rev.*, 1983, **B28**, 2705.

29. Hassold, G. N. and Holm, E. H., *Comp. Phys.*, 1993, **7**, 7.

30. Bortz, A. B., Kalos, M. H. and Lebowitz, J. L., *J. Comput. Phys.*, 1975, **17**, 10.

31. Mehnert, K. and Klimanek, P., in *Proceedings of the 8th Joint EPS/APS International Conference on Physics Computing*, ed. P. Borcherds, M. Bubak and A. Maksymowicz. Academic Computer Centre, Cyfronet-Krakow, Poland, 1996, p. 57.

32. Safran, B. A., Sahni, P. S. and Grest, G. S., *Phys. Rev.*, 1983, **B28**, 2693.

33. Holm, E. A., Zacharopoulos, N. and Srolovitz, D. J., *Acta mater.*, 1998, **46**, 953.

34. Turnbull, D., *AIME*, 1951, **191**, 661.

35. Raabe, D., *Phil. Mag. A*, 1999, **79**, 2339.

36. Rollett, A. D., in *Proceedings of the Third International Conference on Grain Growth, 1998*, ed. H. Weiland. The Minerals, Metals and Materials Society, TMS Publication, Warrendale, PA, 1998.

37. Rollett, A. D. and Raabe, D., in *The Fourth International Conference on Recrystallization and Related Phenomena, 1999*, ed. T. Sakai and H. G. Suzuki. The Japan Institute of Metals, Sendai, 1999, p. 625.